



ECOSYSTEMS

Antarctic biological soil crusts surface reflectance patterns from landsat and sentinel-2 images

ELIANA L. FONSECA, EDVAN C. DOS SANTOS, ANDERSON R. DE FIGUEIREDO &
JEFFERSON C. SIMÕES

Abstract: The remote sensing techniques must be used to obtain long-term information in remote areas, like the Antarctic continent, to monitor the environmental productivity and its changes. The aim of this work was to analyze the surface reflectance profile patterns for the Antarctic biological soil crusts (algae, lichens, and mosses) in an area of Nelson Island (South Shetland Islands, maritime Antarctic), calculated from Landsat and Sentinel-2 images to identify its similarities and differences due to targets, sensors and acquired date. The surface reflectance values for Antarctic biological soil crusts are similar for those observed for biological soil crusts in other Earth extreme environments, like deserts. In Landsat images, the differences among biological soil crusts surface reflectance were identified at visible and near-infrared wavelengths and for Sentinel-2 images, the differences occur at visible, red-edge and shortwave infrared wavelengths, showing the feasibility of using surface reflectance products to identify these different crusts, despite its inherent pixel spectral mixture. Long-term biophysical parameters from such crusts as retrieved from orbital data is not possible due to very low cloud-free images over the Antarctic, which prevents building a consistent surface reflectance time-series which covers all biological soil crusts growth season.

Key words: biophysical parameters, cross calibration, classification, Google Earth Engine, time-series analysis, vegetation.

INTRODUCTION

A small portion of plants survive in the Antarctic environment and its geographic distribution is related with the environment abiotic factors (Putzke et al. 2015). The harsh climatic conditions restrict the vegetation occurrence to ice-free areas, mainly in the Antarctic continent coastal regions and in the Antarctic maritime islands. Vegetation is limited to a narrow altitude range (up to 150 m above sea level), totaling less than 2% of the entire surface of the Antarctic continent (Alberdi et al. 2002, Convey 2006, Fretwell et al. 2011), its growing season length depends on

the climate, latitude, relief and nature of the substrate (Selkirk & Skotnicki 2007).

The Antarctic vegetation is characterized by its seasonality, presenting a complex cycle, related with a set of environmental factors that influence the propagation, germination, growth, the formation of spores and propagules, as well as the establishment of cryptogamic communities (Lewis-Smith 2007). The Antarctic flora consists mainly of inferior plants, with occurrence of cyanobacteria, terrestrial and aquatic algae (700 species), bryophytes - mosses (100 species) and liverworts (25 species) and lichens (250 species) and only two species of vascular plants

(grasses) (Alberdi et al. 2002, Peat et al. 2007). The environmental factors such as temperature, snow cover, winds, daylength, anthropogenic activity and the presence of animals also affect the growth and spatial distribution of vegetation in the maritime Antarctic (Alberdi et al. 2002). The solar radiation reaches the Antarctic surface only in summer months and in this brief period, the vegetation growth is also limited by the existing snow cover, which melts until the middle of the summer season. In polar terrestrial environments, water is available for the vegetation during few months of the year, when snow melts and summers rain occurs or when the air-vapor humidity is absorbed directly from the air (Elster 2002). The availability of water in its liquid state is the most important factor for the development of all vegetation cover communities in Antarctic (Kovacik & Pereira 2001, Elster 2002). The moisture contributes to the establishment of these communities, from spores and propagules dispersed by the wind circulation and animal activities (Bölter et al. 2002).

Biological Soil Crusts (BSC) embrace communities formed by the association of soil particles with microorganisms, such as cyanobacteria, green algae, fungi, lichens, liverworts and mosses. The BSC are able to survive under extreme conditions, for instance, in arid and semi-arid environments, at high temperatures (above 70 °C) or negative ones during most of the year, at high pH levels and high salinities (Karnieli 1997). The BSC have their metabolism and physiological functionality highly dependent on air temperature and air humidity. These set of characteristics makes the BSC as indicators of environmental quality (Ustin et al. 2008, Jensen 2006, Alonso et al. 2014).

The Landsat images were used successfully in studies about BSC in other Earth regions (Karnieli et al. 2001, Chen et al. 2005, Zhang et

al. 2007, Alonso et al. 2014). Once the BSC are environmental quality indicators (Ustin et al. 2008, Jensen 2006, Alonso et al. 2014), monitoring their temporal and spatial dynamic is crucial to a better understood about changes in Antarctic environment. The use of remote sensing data to map and obtain information about Antarctica vegetation is scarce and concentrated mostly on areas frequently visited by researchers (Calviño-Cancela & Martin-Herrero 2016). Those works are usually made with very high resolution images collected by orbital sensors, like KOMPSAT-2 and QuickBird (Shin et al. 2014) and WorldView-2 (Jawak et al. 2019), sometimes in association with information collected by unmanned aerial vehicles (UAV) (Miranda et al. 2020) focused on detecting the vegetation presence or absence in each pixel using Normalized Difference Vegetation Index (NDVI) values. In the era of popular remote sensing the widespread use of NDVI carry inherent risks of misuse by end users who received little remote sensing education (Shin et al. 2014, Huang et al. 2021), sometimes generating an isolated map with information valid only for the image acquisition moment. But the remote sensing techniques must be used not only to generate thematic maps, but also to obtain long-term information from remote areas, like the entire Antarctic continent, allowing to monitor its environment at low costs and in a secure way, without exposing people to extreme environment intrinsic risks. The aim of this work was to analyze the surface reflectance profile patterns for the Antarctic BSC (algae, lichens and mosses) calculated from Landsat and Sentinel-2 images to identify its similarities and differences due targets, environment, sensors and acquired date, in order to use these images in a long-term studies about Antarctic BSC biophysical parameters.

MATERIALS AND METHODS

Study site and fieldwork

The Harmony Point ($62^{\circ}18'S$; $5^{\circ}14'W$) has an area approximately 3.63 km^2 , located in the west coast of Nelson Island, South Shetland Islands, maritime Antarctica (Figure 1), and it is a part of Antarctic Specially Protected Area 133 (ASP 133, http://documents.ats.aq/recatt/Att510_e.pdf). Harmony Point shows three well defined units: an andesitic plateau, which reaches 40 meters above sea level, coastal and shelf outcrops and ancient sea levels raised beaches. There are some extensive areas covered by a very rich and diverse development of bryophytes-mosses (Figure 2a) and lichen-dominated (Figure 2b) plant communities, as well as terrestrial macroscopic green algae communities (Figure 2c). The climate is characterized by mean annual temperatures of approximately $-2.3 \text{ }^{\circ}\text{C}$ and precipitation between 350 and 500 mm per year (Øvstedal & Smith 2001), classified as Polar Marine (Em) according with Köppen classification. The fieldwork was carried out from 13 to 20 February, 2015. Were collected samples at 23 points (Figure 1), in different microenvironments, considering the relief gradient. For each point we collected

the geographic coordinates, elevation and soil cover information.

Dataset

Were used two Landsat images (ETM+ and OLI sensors), Surface Reflectance Level-2 Data Products, which are available from USGS (<http://earthexplorer.usgs.gov>). These images available over path/row 217/104, were acquired on January 19, 2003 by Landsat 7 (ETM+ sensor) and March 17, 2015 by Landsat 8 (OLI sensor), being the cloud-free as criteria to selection. The Surface Reflectance products were georeferenced ready and provide an estimate of the surface spectral reflectance as it would be measured at ground level (atmospheric corrected). But, due to the lack of accuracy about the georeference, both images were co-registered manually, using Landsat 8 image as reference.

Two cloud-free Surface Reflectance Sentinel-2B (MSI sensor) images acquired over the study area on February 23, 2019 and January 19, 2020, available at Google Earth Engine (Gorelick et al. 2017), were used. The Surface Reflectance Sentinel-2 product was obtained from European Union/ESA/Copernicus, at COPERNICUS/S2_SR collection, which contains the surface reflectance values calculated for each Sentinel-2 spectral

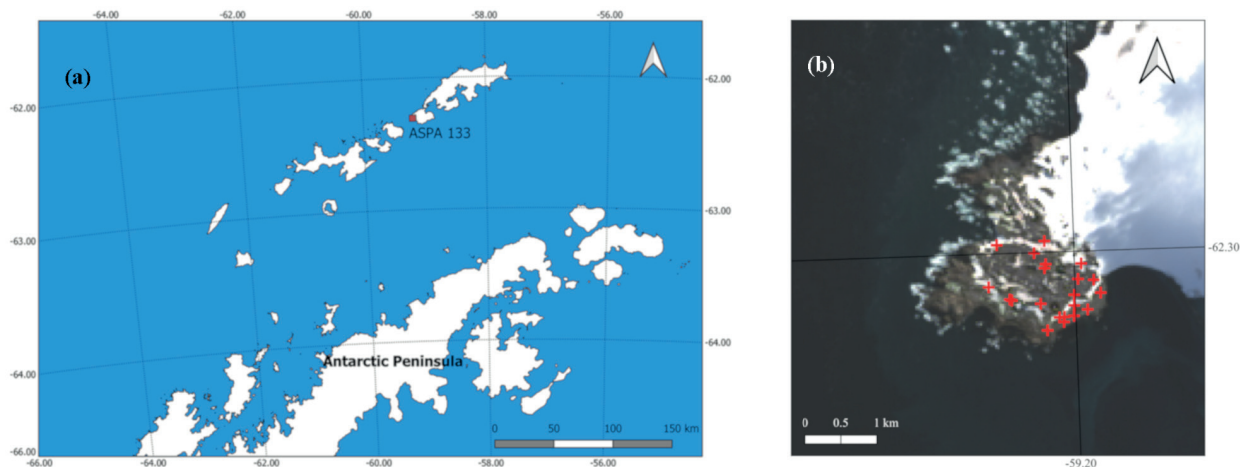


Figure 1. Study area location. The ASP 133 location in relation to the Antarctic Peninsula (a) and samples points over Harmony Point in Nelson Island (b).

bands and three QA bands (quality assessment) that allow assess ice-free and cloud-free pixels only.

Meteorological data, such as daily precipitation and mean air temperature, were used to discuss the differences between surface reflectance patterns. Were used 2m air temperature daily averages and daily total precipitation, collected for the beginning of the

climatic summer season (December 1st) until the image acquisition day. These data were obtained using the Google Earth Engine (Gorelick et al. 2017), from ECMWF/Copernicus Climate Change Service Dataset Provider, ERA5 DAILY collection, which provides aggregated values for each day from ERA5 climate reanalysis parameters.

The vector database in shapefile format, as the Antarctic coastline and the ASPA 133 limits, were downloaded from Antarctic Digital Database Map Viewer (<http://www.add.scar.org>).

Surface reflectance vegetation profiles

To generate average surface reflectance profiles for each BSC, all the six Landsat optical bands located at blue, green, red, near infrared (NIR) and shortwave infrared (SWIR) and also all the ten Sentinel-2 optical bands located at blue, green, red, red edge, NIR and SWIR wavelengths were used (Table I). For the correspondent pixel over the sample point location were collected surface reflectance data. To avoid spectral reflectance mixture at the subpixel level (Shimabukuro & Smith 1991), only those sample points with one target inside the pixel were analyzed. For this approach, a visual analysis was carried out to discard those spectral profiles with reflectance values similar to rocks, ice or water. A t-test was used to compare the reflectance patterns from different years and sensors, comparing the reflectance arithmetic mean for each BSC between Landsat and Sentinel-2 data and between the Landsat images collected in different years, using bands with spectral resolution similar for both sensors (Table I). The minimum level of significance adopted was 10% to infer about the similarity of the data, due to the great natural variability of the Antarctic environment. The low samples amount collected over the Sentinel-2 images in both years prevented the means comparison tests for between these images.

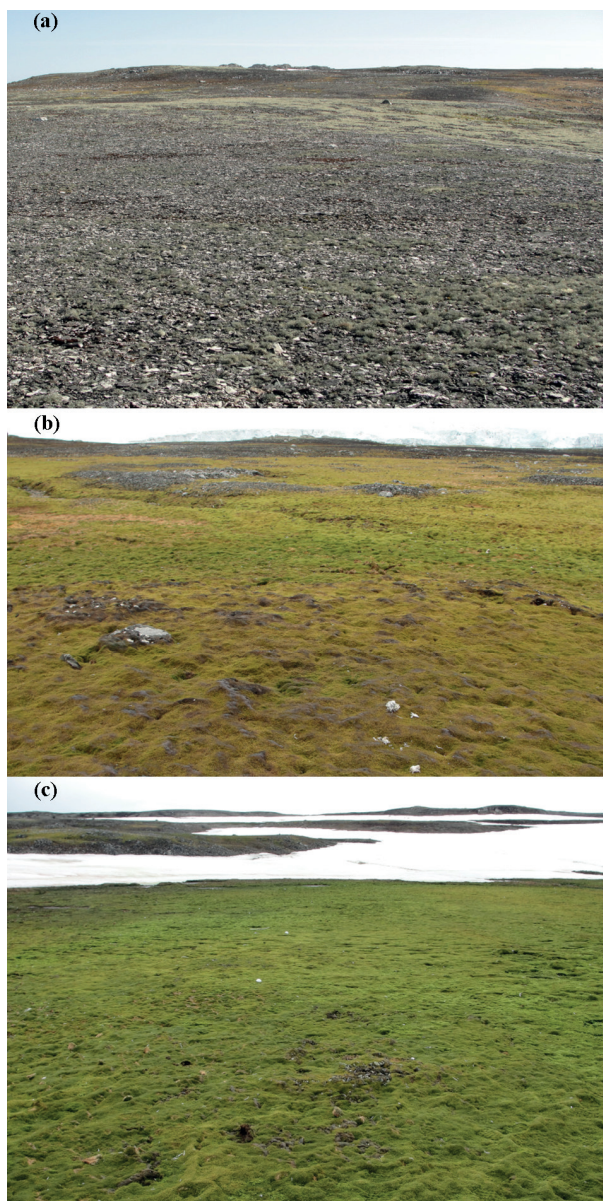


Figure 2. Harmony Point, Nelson Island, photographs showing different biological soil crusts: lichens (a), mosses (b) and algae (c).

Table I. Wavelength name, satellite spectral bandwidth, band number and spatial resolution for ETM+, OLI and MSI(Sentinel-2B) sensors.

Wavelength	Bandwidth / Band number (micrometers)			Resolution (meters)	
	ETM+ ⁽¹⁾	OLI ⁽²⁾	MSI ⁽³⁾	ETM+ / OLI	MSI
Blue	0.450-0.515 / B1	0.452-0.512 / B2	0.426-0.558 / B2	30	10
Green	0.525-0.605 / B2	0.533-0.590 / B3	0.523-0.595 / B3	30	10
Red	0.630-0.690 / B3	0.636-0.673 / B4	0.634-0.696 / B4	30	10
Red Edge	-	-	0.688-0.720 / B5	-	20
	-	-	0.724-0.754 / B6	-	20
	-	-	0.760-0.800 / B7	-	20
NIR	0.775-0.950 / B4	0.851-0.879 / B5	0.727-0.939 / B8	30	10
	-	-	0.842-0.886 / B8A	-	20
SWIR	1.550-1.750 / B5	1.566-1.651 / B6	1.516-1.705 / B11	30	20
	2.080-2.350 / B7	2.107-2.294 / B7	2.001-2.371 / B12	30	20

(1)<https://www.usgs.gov/media/files/landsat-7-data-users-handbook>; (2)<https://www.usgs.gov/media/files/landsat-8-data-users-handbook>; (3)<https://sentinel.esa.int/web/sentinel/user-guides/sentinel-2-msi/resolutions/radiometric>.

RESULTS

The Figure 3 shows the average surface reflectance patterns for Antarctic BSC, namely, green algae, lichens and mosses collected over Landsat and Sentinel-2 images. For Landsat images (Figure 3a) the surface reflectance patterns present low values, with maximum values around 0.25 in all wavelengths and the differences among Antarctic BSC surface reflectance occur at visible and NIR wavelengths, while at the SWIR wavelengths they present similar values. For Sentinel-2 images (Figure 3b) the surface reflectance patterns also present low values, with maximum values around 0.25 in all wavelengths and the differences among Antarctic BSC surface reflectance occur at visible, red edge and SWIR wavelengths.

The Tables II, III and IV shows the mean surface reflectance values for the analyzed sensors and years in Landsat and Sentinel-2 images and the t-test results for the equal means hypothesis for algae, lichens and mosses. Once the images were acquired in different months,

the accumulated temperature above zero (water melting point) were also different and some sample points were under a snow cover, resulting in different sample points numbers (n) for each year. For the comparison tests between Landsat sensors/years and between Landsat and Sentinel-2 surface reflectance average were found statistical differences at various wavelengths, using 10% as minimum level of probability, being these differences also dependent on with analyzed target.

DISCUSSION

Surface reflectance patterns for Antarctic BSC in Landsat images

The Antarctic BSC average reflectance patterns observed in Landsat images (Figure 3a) are similar to patterns describes for BSC in Landsat images from other Earth's environments, like desert areas (Chen et al. 2005, Zhang et al. 2007), being as evidence about BSC physiology adaptation (Thomas & Wiencke 1991) to extreme environments conditions over a wide

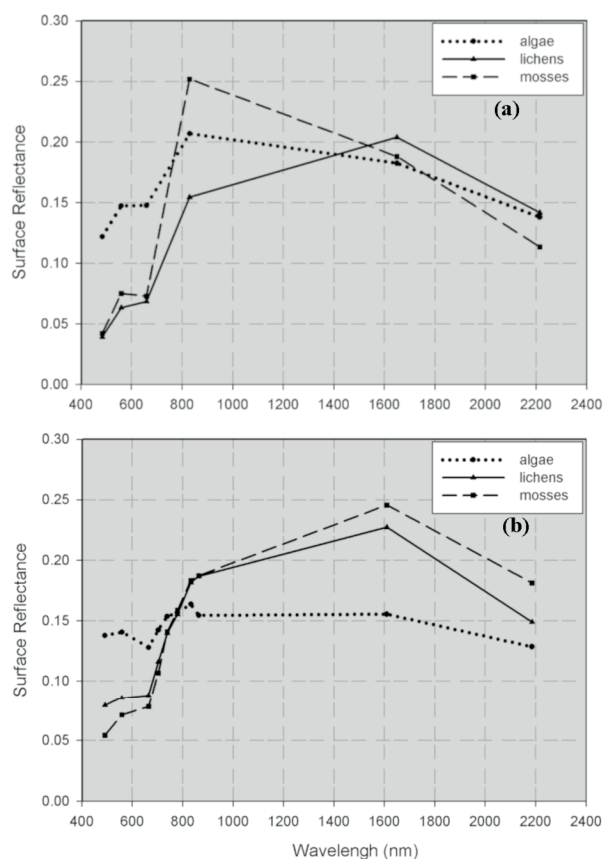


Figure 3. Average reflectance patterns for biological soil crusts from Landsat (a) and Sentinel-2 (b) images.

temperature range. Specifically for the visible wavelengths (the same wavelengths related with radiation absorbed by the photosynthesis process) the reflectance values observed for each BSC at the green and red wavelengths are similar while at the blue wavelengths are lower, these BSC's patterns are also observed in other environments (Karnieli 2003, Chen et al. 2005, Zhang et al. 2007) and with spectroradiometer experiments (Bechtel et al. 2002, Calviño-Cancela & Martin-Herrero 2016).

The algae surface reflectance pattern shows values around 0.15 at all wavelengths (Figure 3a), presenting higher values than lichens and mosses in visible wavelengths. Previous works about Antarctic algae reflectance patterns were focus on snow algae (Painter et al. 2001, Gray et al.

2020) and this fact explain the differences found for reflectance patterns in SWIR wavelengths. All the incoming electromagnetic radiation at the SWIR wavelengths reaching free water, ice and snow are absorbed (Jensen 2006) and they act as a strong background signal in pixel spectral mixture (Shimabururo & Smith 1991) detected by orbital sensors, resulting reflectance values near zero for snow algae pixels dominated (Painter et al. 2001, Gray et al. 2020). In the Antarctic terrestrial environment, macroscopic green algae occur in moist areas (Becker 1982, Jacob et al. 1991, Broady 1996, Kovacic & Pereira 2001), growing over a very thin water layer which have few influence as a background signal in pixel spectral mixture, resulting in surface reflectance values different from zero (Figure 3a), despite this water layer alters the vegetation surface reflectance values.

Higher reflectance values were observed for mosses at NIR wavelengths (Figure 3a), presenting similarity with a green leaf reflectance pattern and have also been observed in other studies (Lovelock & Robinson 2002, Zhang et al. 2007). Despite mosses leaves are formed by a single layer cells, without a mesophyll structure (Waite & Sack 2010), their leaves layers can increase the reflectance at the NIR wavelengths. Since in the Antarctic environment the reproduction occurs asexually for all mosses, due to the limiting conditions of the local environment (Kappen & Schroeter 2002), the mosses morphology presents gametophyte patterns, with axis that supports phyllids (leaf-like structures), arranged in a spiral (Waite & Sack 2010) and these structure can be simulated a vascular leaf reflectance pattern, with an increase at the NIR wavelengths.

Different from mosses and algae, lichens have their surface reflectance peak in the SWIR wavelength in Landsat images (Figure 3a), also observed with spectroradiometer

Table II. Algae mean surface reflectance values for Landsat and Sentinel-2, number of samples and result of the t-test between Landsat sensors (A) and between the averages of both satellites (B).

Wavelength	2003 / Landsat - ETM+ (n = 7)	2015/ Landsat - OLI (n = 4)	T-test (p value) - A	2019 / Sentinel - MSI (n = 3)	2020 / Sentinel - MSI (n = 2)	Landsat (average) (n = 11)	Sentinel (average) (n = 5)	T-test (p value) -B
Blue	0.115*	0.132*	0.3118	0.126	0.156	0.122#	0.138#	0.2177
Green	0.137	0.162	0.0286	0.121	0.170	0.147#	0.140#	0.9463
Red	0.133	0.170	0.0024	0.108	0.158	0.148#	0.128#	0.2908
NIR	0.203*	0.212*	0.5394	0.132	0.210	0.207	0.164	0.0162
SWIR	0.225	0.118	0.0021	0.109	0.224	0.182#	0.155#	0.3669
SWIR	0.173	0.086	0.0015	0.088	0.188	0.138#	0.128#	0.7003

Landsat surface reflectance means following by * in the same wavelength have no statistical difference using a 10% as minimum level of probability. Surface reflectance means following by # in the same wavelength for comparison between satellites have no statistical difference using a 10% as minimum level of probability.

measurement by Casanovas et al. (2015). Lichens showed a pattern of low reflectance values at all wavelengths and poor absorption of the red wavelength by photosynthesis process, being similar with laboratory measurements made by Bechtel et al. (2002). Lichens and mosses have a similar pattern at the visible wavelengths, but at the sub pixel level, lichens dominated pixels presents the dark rock background (Shin et al. 2014, Calviño-Cancela & Martin-Herrero 2016) also compounding the signal detected by the sensor, due to the Landsat spatial resolution and the sparse coverage of the lichens in most of the sites.

Antarctic BSC surface reflectance similarities and differences due sensors

The Antarctic BSC average surface reflectance patterns observed in Sentinel-2 images (Figure 3b) show some similarities when they are compared to patterns observed in Landsat images (Figure 3a). Algae show low reflectance values, around 0.15, at all wavelengths and higher values than lichens and mosses at visible wavelengths. For lichens and mosses were observed the same similarity at visible

wavelengths for Sentinel-2 and Landsat images, indicating that they are not distinguishable in these wavelengths, but indicate the feasibility to identify terrestrial algae in ice-free areas in both Landsat and Sentinel-2 images using a simple classification image procedure.

For mosses were observed a distinct reflectance peak related with satellite, which occur at SWIR wavelength for Sentinel-2 and at NIR for Landsat (Table IV), and this can be attributed to the great difference among NIR bandwidth for different sensors (Table I). In fact, the differences of surface reflectance values between Landsat and Sentinel-2 images and between Landsat images acquired in different years (Tables II, III and IV) were expected because they were acquired from different sensors (also observed by Flood 2014, 2017, Roy et al. 2016 among others). Each sensor is a set of detectors, calibrated in a uniform way to generate consistently images from Earth's surface, and has its own "spectral response function" for each spectral band (Trishchenko et al. 2002, Gonsamo & Chen 2013, Barsi et al. 2014) producing a different output signal for the

Table III. Lichens average surface reflectance values for Landsat and Sentinel-2, number of samples and result of the t-test between Landsat sensors (A) and between the averages of both satellites (B).

Wavelength	2003 / Landsat - ETM+ (n = 2)	2015/ Landsat - OLI (n = 3)	t-test (p value) - A	2019 / Sentinel - MSI (n = 2)	2020 / Sentinel - MSI (n = 2)	Landsat (average) (n = 5)	Sentinel (average) (n = 4)	t-test (p value) -B
Blue	0.034*	0.043*	0.2199	0.104	0.053	0.039	0.079	0.0353
Green	0.064*	0.063*	0.4851	0.098	0.073	0.063	0.085	0.0991
Red	0.078*	0.062*	0.1841	0.090	0.086	0.069#	0.088#	0.1031
NIR	0.175	0.141	0.0451	0.137	0.226	0.154#	0.181#	0.3273
SWIR1	0.276	0.155	0.0009	0.123	0.331	0.204#	0.227#	0.7203
SWIR 2	0.195	0.106	0.0029	0.098	0.200	0.142#	0.149#	0.8517

Landsat surface reflectance means following by * in the same wavelength have no statistical difference using 10% as minimum level of probability. Surface reflectance means following by # in the same wavelength for comparison between satellites have no statistical difference using 10% as minimum level of probability.

same target under the same image acquisition geometry and illumination conditions.

As the BSC surface reflectance patterns for red and NIR wavelengths in both satellites (Figure 3) are different from the other targets at surroundings, like snow and rocks (Winther 1993, Jensen 2006, Kang et al. 2018, Vaudour et al. 2019), a classification procedure using these bands alone, or combined by Normalized Difference Vegetation Index (NDVI), as input data can generate a valid vegetation thematic map (Murray et al. 2010, Fretwell et al. 2011, Vieira et al. 2014, Shin et al. 2014, Casanovas et al. 2015, Jawak et al. 2019, Miranda et al. 2020, Sotille et al. 2020). These vegetation maps, although statistically valid, are not comparable to each other, being valid only for that specifically image and for the same study area, due environmental factors like precipitation and the BSC phenological stage that alters the BSC signal detected by orbital sensors (Fang et al. 2015, Zhao et al. 2017, Lehnert et al. 2018), because the free water over surface alters the reflectance values (as observed in Tables II, III and IV) and, consequently, the NDVI values (Wang et al. 2003, Pei et al. 2019). Neither the parameters for generating the map, such as end members definition for spectral mixture analyzes, nor descriptive statistics can

be used to generate a similar map with an image acquired on any other date.

The cross-calibration among different sensors, mandatory before build a surface reflectance or NDVI time-series based on satellite images, is not feasible in Antarctic due the very low number of cloud-free images, as can be notice by the large temporal lag between the two Landsat images analyzed in this work. From 2003 to 2015, no other cloud-free images were collected over the study area by any Landsat satellite. This particular condition prevents a long term analysis of BSC biophysical parameters based on their surface reflectance pattern collected over satellite images. Some parameters like fraction of photosynthetically active radiation absorbed (FAPAR), which is an essential climate variable required for the monitoring and modeling of land surfaces (Baret et al. 2013), also required to calculate the ecosystem gross primary production based on light use efficiency concept (Monteith 1972), cannot be estimate by synergistic use of Landsat and Sentinel-2 for Antarctic vegetation due the its sensors intrinsic differences and the impossibility of cross-calibration.

Even when use only Sentinel-2 images to build a surface reflectance time-series, a

Table IV. Mosses average surface reflectance values for Landsat and Sentinel-2, number of samples and result of the t-test between Landsat sensors (A) and between the averages of both satellites (B).

Wavelength	2003 / Landsat - ETM+ (n = 7)	2015/ Landsat - OLI (n = 11)	t-test (p value) - A	2019 / Sentinel - MSI (n = 3)	2020 / Sentinel - MSI (n = 3)	Landsat (average) (n = 18)	Sentinel (average) (n = 6)	t-test (p value) -B
Blue	0.048*	0.040*	0.31272	0.068	0.040	0.042#	0.054#	0.2451
Green	0.081*	0.072*	0.13732	0.074	0.068	0.075#	0.071#	0.7156
Red	0.086	0.067	0.04806	0.072	0.084	0.073#	0.078#	0.6569
NIR	0.285*	0.237*	0.21083	0.144	0.223	0.252	0.183	0.0190
SWIR1	0.295	0.140	0.00009	0.131	0.360	0.188#	0.246#	0.2382
SWIR 2	0.195	0.077	0.00024	0.108	0.254	0.113	0.181	0.0727

Landsat surface reflectance means following by * in the same wavelength have no statistical difference using 10% as minimum level of probability. Surface reflectance means following by # in the same wavelength for comparison between satellites have no statistical difference using 10% as minimum level of probability.

cross-calibration is necessary because the MSI sensor on board at Sentinel-2A is different from MSI sensor on Sentinel-2B. Specifically about the Sentinel-2 images accessed by Google Earth Engine, a standard search returns a set of images without informing whether they were collected by Sentinel 2A or 2B, being necessary to retrieve this information from the imagery metadata with a properly command line. Also, due the granules overlap, the same ground area distributed in different granules presenting different surface reflectance values (Table V), despite being collected during the same satellite (Sentinel-2B) overpass. It occurs because the atmospheric correction parameters used are the same for an entire granule, but different for each granule, as can be observing in the image metadata, generating different surface reflectance values (Table V) for the same pixel. For retrieving information about vegetation biophysical parameters from satellite images, like aboveground biomass, is necessary field measurements made at the same image acquired day, or with a minimum leg of two days, that will be related with surface reflectance values over same pixel where the sample was collected. Using the Google Earth Engine to build a surface reflectance time-series, even are selected

only images from Sentinel-2A or Sentinel-2B, the reduce command chosen to combine the different values from different granules affect the time-series values. When exists many NDVI values over same area, a common approach is used the maximum NDVI value composite (Holben 1986), but it is used for various images collected in different days or in different day-time. The use of surface reflectance maximum value composite to reduce values from different Sentinel-2 granules available in Google Earth Engine will take data from different granule for each wavelength (Table V). On the other hand the use surface reflectance mean value will generate values different from those originally collected, generating some difficulty to obtain a consistent surface reflectance time-series values.

Surface reflectance changes due environmental factors

Some differences in BSC reflectance values observed between Landsat images acquired in years 2003 and 2015 can be explained by the time of year when the image was acquired, that defines the meteorological data and vegetation phenological stage. In January 19, 2003 the sum of daily mean air temperature since December

Table V. Surface reflectance values from Sentinel-2B estimated for granules T21EUL and T21EUM for the same satellite overpass over study area.

Granule	Band ID									
	B2	B3	B4	B5	B6	B7	B8	B8A	B11	B12
T21EUL	0.078	0.09	0.091	0.115	0.139	0.149	0.152	0.16	0.149	0.126
T21EUM	0.075	0.087	0.088	0.115	0.143	0.154	0.161	0.167	0.15	0.125

1st, 2002 was 29.2 °C while in March 17, 2015 the same sum since December 1st, 2014 was 66.2 °C. As the BSC growing season length is defined by air temperature, differences in photosynthesis rate (Yoshitake et al. 2010) and, consequently, in surface reflectance are expected as the BSC becomes more developed (Karnieli 2003, Sancho & Pintado 2004), presenting a lower reflectance and well defined absorbed bands, as can be noticed when compared the image acquired late in the growing season (March) with the image acquired at the beginning of growing season (January), at red, NIR and SWIR wavelengths for lichens (Table III) and mosses (Table IV).

The differences in surface reflectance values observed for algae between 2003 and 2015 (Table II) can be explained by the total precipitation amount in the days before image acquisition, which promotes differences in available free water over the surface. In the week before image acquisition the total precipitation amount was 27 mm in 2003 and 46 mm in 2015, and in the four days before image acquisition the total precipitation amount was 0 mm in 2003 and 29 mm in 2015, resulting in changes in vegetation reflectance patterns (Karnieli et al. 1999, Bechtel et al. 2002, Ustin et al. 2008, Chamizo et al. 2012, Weber & Hill, 2016), as the algae are often locate on pools of water (Putzke & Pereira 2020) and, in this case, the water acting as a background, reducing the surface reflectance values in both SWIR bands and moving the reflectance peak from SWIR in 2003 to NIR in 2015 (Table II). This kind of behaviour

were also observed for mosses (Table IV), which also grow in moist microenvironments.

Despite the low number of samples that prevents the use a t-test to compare means, some differences in BSC reflectance values were observed between Sentinel-2 images acquired in years 2019 and 2020 and they can also be explained by the image acquired month. The sum of daily mean air temperature from the beginning of meteorological summer season (December 1st) was 58.0 °C in February 23, 2019, greater than 34.8 °C observed in January 19, 2020. No precipitation events were observed in the seven days before the acquisition of both images. For all BSC were observed lower surface reflectance values for NIR and SWIR in February than in January (Tables II, III and IV). The environmental factors that can be cited to explain these variations are the more free water available over the surface, due a greater accumulated air temperature that occurs in February. When compared surface reflectance values for algae (Table II) and mosses (Table IV) the lower values observed in February are due a great green biomass amount, which define a great photosynthesis rate (Yoshitake et al. 2010) and, consequently, a reduce in surface reflectance values as BSC becomes more developed (Karnieli 2003, Sancho & Pintado 2004).

The observed differences due meteorological conditions and in association with the few cloud-free images over Antarctic region during the BSC growth season do not allow a direct comparison

on biomass accumulation or the retrieving any other vegetation biophysical parameter from satellite images. As observed by Shin et al. (2014), there are variations of vegetation abundance related to the acquired month and interannual meteorological conditions variations, although the vegetation distribution area detected by satellite images does not change. Only a consistent long surface reflectance time-series, built with images collected during the all BSC growth season in different years will allow retrieving the Antarctic vegetation biophysical parameters using remote sensing techniques.

CONCLUSIONS

The surface reflectance values for Antarctic BSC calculated from Landsat and Sentinel-2 surface reflectance products are similar with those observed for BSC from other Earth's extreme environment. In Landsat images, the differences among Antarctic BSC surface reflectance were identified at visible and NIR wavelengths and for Sentinel-2 images the differences occur at visible, red-edge and SWIR wavelengths. These differences show the feasibility of using surface reflectance products from orbital sensors with 20-30m of spatial resolution to identify the different BSC in the Antarctic environment, despite the inherent spectral mixture at the sub-pixel level, being possible if all available spectral information are used for the classification process. It not feasible to retrieve Antarctic BSCs biophysical parameters from orbital data by the synergistic use of Landsat and Sentinel-2 images due very low number of cloud-free images over the maritime Antarctic, preventing the cross-calibration among satellites sensors. The same reason prevents to build a consistent surface reflectance time-series using only Sentinel-2 images, as it is impossible to obtain cloud-free images for all BSC growth season.

Acknowledgments

This work was supported financially by Conselho Nacional de Desenvolvimento Científico e Tecnológico (CNPq) - Process 465680/2014-3 and the Fundação de Amparo à Pesquisa do Estado do Rio Grande do Sul (FAPERGS) - Process 17/25510000518-0 through the Brazilian National Institute for Cryospheric Sciences (INCT da Criosfera).

REFERENCES

- ALBERDI M, BRAVO LA, GUTIÉRREZ A, GIDEKEL M & CORCUERA LJ. 2002. Ecophysiology of Antarctic vascular plants. *Physiol Plantarum* 115: 479-486.
- ALONSO M, RODRÍGUEZ-CABALLERO E, CHAMIZO S, ESCRIBANO P & CANTÓN Y. 2014. Evaluación de los diferentes índices para cartografiar biocostras a partir de información espectral. *Revista Española de Teledetección* 42: 79-98.
- BARET F, WEISS M, LACAZE R, CAMACHO F, MAKHMARA H, PACHOLCYZK P & SMETS B. 2013. GEOV1: LAI and FAPAR essential climate variables and FCOVER global time series capitalizing over existing products. Part1: Principles of development and production. *Remote Sens Environ* 137: 299-309.
- BARSI JA, LEE K, KVARAN G, MARKHAM BL & PEDELTY JA. 2014. The Spectral Response of the Landsat-8 Operational Land Imager. *Remote Sens* 6: 10232-10251.
- BECHTEL R, RIVARD B & SANCHEZ-AZOFEIFA A. 2002. Spectral properties of foliose and crustose lichens based on laboratory experiments. *Remote Sens Environ* 82: 389-396.
- BECKER EW. 1982. Physiological studies on Antarctic *Prasiola crispa* and *Nostoc commune* at low temperatures. *Polar Biol* 1: 99-104.
- BÖLTER M, BEYER L & STONEHOUSE B. 2002. Antarctic coastal landscapes: characteristics, ecology and research. In: Beyer L & Bölter M (Eds), *Geocology of Antarctic ice-free coastal landscapes*, Berlin: Springer-Verlag, p. 5-15.
- BROADY PA. 1996. Diversity, distribution and dispersal of Antarctic terrestrial algae. *Biodivers Conserv* 5: 1307-1335.
- CALVIÑO-CANCELA M & MARTÍN-HERRERO J. 2016. Spectral Discrimination of Vegetation Classes in Ice-Free Areas of Antarctica. *Remote Sens* 8: 856.
- CASANOVAS P, BLACK M, FRETWELL P & CONVEY P. 2015. Mapping lichen distribution on the Antarctic Peninsula using remote sensing, lichen spectra and photographic documentation by citizen scientists. *Polar Res* 34: 25633.

- CHAMIZO S, STEVENS A, CANTÓN Y, MIRALLES I, DOMINGO F & VAN WESEMAEL B. 2012. Discriminating soil crust type, development stage and degree of disturbance in semiarid environments from their spectral characteristics. *Eur J Soil Sci* 63: 42-53.
- CHEN J, ZHANG MY, WANG L, SHIMAZAKIA H & TAMURA M. 2005. A new index for mapping lichen-dominated biological soil crusts in desert areas. *Remote Sens Environ* 96: 165-175.
- CONVEY P. 2006. Antarctic terrestrial ecosystems: responses to environmental change. *Polarforschung* 75: 101-111.
- ELSTER J. 2002. Ecological classification of terrestrial algal communities in polar environments. In: Beyer L & Bölter M (Eds), *Geoecology of Antarctic ice-free coastal landscapes*, Berlin: Springer-Verlag, p. 303-326.
- FANG S, YU W & QI Y. 2015. Spectra and vegetation index variations in moss soil crust in different seasons, and in wet and dry conditions. *Int J Appl Earth Obs Geoinf* 38: 261-266.
- FLOOD N. 2014. Continuity of reflectance data between Landsat-7 ETM+ and Landsat-8 OLI, for both top-of-atmosphere and surface reflectance: a study in the Australian landscape. *Remote Sens* 6: 7952-7970.
- FLOOD N. 2017. Comparing Sentinel-2A and Landsat 7 and 8 using surface reflectance over Australia. *Remote Sens* 9: 659.
- FRETWELL PT, CONVEY P, FLEMING AF, PEAT HJ & HUGHES KA. 2011. Detecting and mapping vegetation distribution on the Antarctic Peninsula from remote sensing data. *Polar Biol* 34: 273-281.
- GONSAMO A & CHEN JM. 2013. Spectral Response Function Comparability Among 21 Satellite Sensors for Vegetation Monitoring. *IEEE Trans Geosci Remote Sens* 51: 1319-1335.
- GORELICK N, HANCHER M, DIXON M, ILYUSHCHENKO S, THAU D & MOORE R. 2017. Google Earth Engine: Planetary-scale geospatial analysis for everyone. *Remote Sens Environ* 202: 18-27.
- GRAY A, KROLIKOWSKI M, FRETWELL P, CONVEY P, PECK LS, MENDELOVA M, SMITH AG & DAVEY MP. 2020. Remote sensing reveals Antarctic green snow algae as important terrestrial carbon sink. *Nat Commun* 11: 2527.
- HOLBEN BN. 1986. Characteristics of maximum-value composite images from temporal AVHRR data. *Int J Remote Sens* 7: 1417-1434.
- HUANG S, TANG L, HUPY JP, WANG Y & SHAO G. 2021. A commentary review on the use of normalized difference vegetation index (NDVI) in the era of popular remote sensing. *J For Res* 32: 1-6.
- JACOBA, KIRST GO, WIENCKE C & LEHMANN H. 1991. Physiological responses of the Antarctic green alga *Prasiola crispa* ssp. *antarctica* to salinity stress. *J Plant Physiol* 139: 57-62.
- JAWAK SD, LUIS AJ, FRETWELL PT, CONVEY P & DURAIRAJAN UA. 2019. Semiautomated detection and mapping of vegetation distribution in the Antarctic environment using spatial-spectral characteristics of Worldview-2 imagery. *Remote Sens* 11: 1909.
- JENSEN JR. 2006. *Remote sensing of the environment: An Earth resource perspective*. Upper Saddle River, NJ: Prentice Hall, 592 p.
- KANG J, CHENG X, HUI F & CI T. 2018. An accurate and automated method for identifying and mapping exposed rock outcrop in Antarctica using Landsat 8 images. *IEEE J Sel Top Appl Earth Obs Remote Sens* 11: 57-67.
- KAPPEN L & SCHROETER B. 2002. Plants and Lichens in the Antarctic, Their Way of Life and Their Relevance to Soil Formation. In: Belnap J & Lange OL (Eds), *Biological soil crusts: structure, function, and management*. 150. *Ecological Studies (Analysis and Synthesis)*. Berlin: Springer, p. 327-373.
- KARNIELI A. 1997. Development and implementation of spectral crust index over dune sands. *Int J Remote Sens* 18: 1207-1220.
- KARNIELI A. 2003. Natural vegetation phenology assessment by ground spectral measurements in two semi-arid environments. *Int J Biometeorol* 47: 179-187.
- KARNIELI A, KIDRON GJ, GLAESSER C & BEN-DOR E. 1999. Spectral characteristics of cyanobacteria soil crust in semiarid environments. *Remote Sens Environ* 69: 67-75.
- KARNIELI A, KOKALY RF, WEST NE & CLARK RN. 2001. Remote sensing of biological soil crusts. In: Belnap J & Lange OL (Eds), *Biological soil crusts: structure, function, and management*. 150. *Ecological Studies (Analysis and Synthesis)*. Berlin: Springer, p. 431-455.
- KOVACIK L & PEREIRA AB. 2001. Green alga *Prasiola crispa* and its lichenized form *Mastodia tessellata* in Antarctic environment: general aspects. *Nova Hedwigia Beiheft* 123: 465-478
- LEHNERT LW, JUNG P, OBERMEIER WA, BÜDEL B & BENDIX J. 2018. Estimating net photosynthesis of biological soil crusts in the Atacama using hyperspectral remote sensing. *Remote Sensing* 10: 891.

- LEWIS-SMITH RI. 2007. Vegetation. In: Riffenburgh B (Ed), *Encyclopedia of the Antarctic*. New York: Taylor & Francis Group, p. 1033-1036.
- LOVELOCK CE & ROBINSON SA. 2002 Surface reflectance properties of Antarctic moss and their relationship to plant species, pigment composition and photosynthetic function. *Plant Cell Environ* 25: 1239-1250.
- MIRANDA V, PINA P, HELENO S, VIEIRA G, MORA C & SCHAEFER CEGR. 2020. Monitoring recent changes of vegetation in Fildes Peninsula (King George Island, Antarctica) through satellite imagery guided by UAV surveys. *Sci Total Environ* 704: 135295.
- MONTEITH J. 1972. Solar radiation and productivity in tropical ecosystems. *J Appl Ecol* 9: 747-766.
- MURRAY H, LUCIEER A & WILLIAMS R. 2010. Texture-based classification of sub-Antarctic vegetation communities on Heard Island. *Int J Appl Earth Obs* 12: 138-149.
- ØVSTEDAL DO & SMITH RIL. 2001. *Lichens of Antarctica and South Georgia: A guide to their identification and ecology*. Cambridge: Cambridge University Press, 453 p.
- PAINTER TH, DUVAL B, THOMAS WH, MENDEZ M, HEINTZELMAN S & DOZIER J. 2001. Detection and quantification of snow algae with an airborne imaging spectrometer. *Appl Environ Microbiol* 67: 5267-5272.
- PEAT HJ, CLARKE A & CONVEY P. 2007. Diversity and biogeography of the Antarctic flora. *J Biogeogr* 34: 132-146.
- PEI Z, FANG S, YANG W, WANG L, WU M, ZHANG Q, HAN W & KHOI DN. 2019. The Relationship between NDVI and climate factors at different monthly time scales: a case study of grasslands in Inner Mongolia, China (1982-2015). *Sustainability* 11: 7243.
- PUTZKE J, ATHANÁSIO CG, ALBUQUERQUE, MP, VICTORIA FC & PEREIRA BA. 2015. Comparative study of moss diversity in South Shetland Islands and in the Antarctic Peninsula. *Rev Chil Hist Nat* 88: 1-6.
- PUTZKE J & PEREIRA BA. 2020. The Vegetation of the South Shetland Islands and the climatic change In: Kanao M (Ed), *Glaciers and the polar environment*. London: IntechOpen, cap 4.
- ROY DP, KOVALSKYY V, ZHANG HK, VERMOTE EF, YAN L, KUMAR SS & EGOROV A. 2016. Characterization of Landsat-7 to Landsat-8 reflective wavelength and normalized difference vegetation index continuity. *Remote Sens Environ* 185: 57-70.
- SANCHO LG & PINTADO A. 2004. Evidence of high annual growth rate for lichens in the maritime Antarctic. *Polar Biol* 27: 312-319.
- SELKIRK PM & SKOTNICKI ML. 2007. Measurement of moss growth in continental Antarctica. *Polar Biol* 30: 407-413.
- SHIMABUKURO YE & SMITH JA. 1991. The least-squares mixing models to generate fraction images derived from remote sensing multispectral data. *IEEE Trans Geosci Remote Sens* 29: 16-20.
- SHIN JI, KIM HC, KIM SI & HONG SG. 2014. Vegetation abundance on the Barton Peninsula, Antarctica: estimation from high-resolution satellite images. *Polar Biol* 37: 1579-1588.
- SOTILLE ME, BREMER UF, VIEIRA G, VELHO LF, PETSCH C & SIMÕES JC. 2020. Evaluation of UAV and satellite-derived NDVI to map maritime Antarctic vegetation. *Appl Geogr* 125: 102322.
- THOMAS DN & WIENCKE C. 1991. Photosynthesis, dark respiration and light independent carbon fixation of endemic Antarctic macroalgae. *Polar Biol* 11: 329-337.
- TRISHCHENKO AP, CIHLAR J & LI Z. 2002. Effects of spectral response function on surface reflectance and NDVI measured with moderate resolution satellite sensors. *Remote Sens Environ*: 81: 1-18.
- USTIN SL, VALKO PG, KEFAUVER SC, SANTOS MJ, ZIMPFER JF & SMITH SD. 2008. Remote sensing of biological soil crust under simulated climate change manipulations in the Mojave Desert. *Remote Sens Environ* 113: 317-328.
- VAUDOURE E, GOMEZ C, FOUAD Y & LAGACHERIE P. 2019. Sentinel-2 image capacities to predict common topsoil properties of temperate and Mediterranean agroecosystems. *Remote Sens Environ* 223: 21-33.
- VIEIRA G, MORA C, PINA P & SCHAEFER CER. 2014. A proxy for snow cover and winter ground surface cooling: Mapping *Usnea* sp. communities using high resolution remote sensing imagery (Maritime Antarctica). *Geomorphology* 225: 69-75.
- WAITE M & SACK L. 2010. How does moss photosynthesis relate to leaf and canopy structure? Trait relationships for 10 Hawaiian species of contrasting light habitats. *The New Phytologist* 185: 156-172.
- WANG J, RICH PM & PRICE KP. 2003. Temporal responses of NDVI to precipitation and temperature in the central Great Plains, USA. *Int J Remote Sens* 24: 2345-2364.
- WEBER B & HILL J. 2016. Remote sensing of biological soil crusts at different scales. In: Weber B, Büdel B & Belnap J (Eds), *Biological soil crusts: an organizing principle in drylands*, 226. *Ecological Studies (Analysis and Synthesis)*, Berlin: Springer, p. 215-234.

WINTHER J. 1993. Landsat TM derived and in situ summer reflectance of glaciers in Svalbard. *Polar Research* 12: 37-55.

YOSHITAKE S, UCHIDA M, KOIZUMI H, KANDA H & NAKATSUBO T. 2010. Production of biological soil crusts in the early stage of primary succession on a High Arctic glacier foreland. *New Phytologist* 186: 451-460.

ZHANG YM, CHEN J, WANG L, WANG XQ & GU ZH. 2007. The spatial distribution patterns of biological soil crusts in the Gurbantunggut Desert, Northern Xinjiang, China. *J Arid Environ* 68: 599-610.

ZHAO Y, JIA R, GAO Y, ZHOU Y & TENG J. 2017. Characteristics of normalized difference vegetation index of biological soil crust during the succession process of artificial sand-fixing vegetation in the Tengger Desert, Northern China. *Chin J Plan Ecol* 41: 972-984.

How to cite

FONSECA EL, SANTOS EC, FIGUEIREDO AR & SIMÕES JC. 2022. Antarctic biological soil crusts surface reflectance patterns from landsat and sentinel-2 images. *An Acad Bras Cienc* 94: e20210596. DOI 10.1590/0001-376520220210596.

*Manuscript received on April 18, 2021;
accepted for publication on November 10, 2021*

ELIANA L. FONSECA¹

<https://orcid.org/0000-0002-9129-2939>

EDVAN C. DOS SANTOS²

<https://orcid.org/0000-0001-8008-2509>

ANDERSON R. DE FIGUEIREDO²

<https://orcid.org/0000-0002-0228-249X>

JEFFERSON C. SIMÕES^{1,3}

<https://orcid.org/0000-0001-5555-3401>

¹Universidade Federal do Rio Grande do Sul, Centro Polar e Climático, Departamento of Geography, Av. Bento Gonçalves, 9500, 91501-970 Porto Alegre, RS, Brazil

²Universidade Federal do Rio Grande do Sul, Centro Polar e Climático, Av. Bento Gonçalves, 9500, 91501-970 Porto Alegre, RS, Brazil

³University of Maine, Climate Change Institute, Bryard Global Sciences Building, 04469-5790, Orono, ME, USA

Correspondence to: **Eliana Lima da Fonseca**

E-mail: eliana.fonseca@ufrgs.br

Author contributions

ELF performed the fieldwork, analyzed the data, wrote, reviewed and edited the manuscript; ECS performed the literature review, analyzed the data and wrote the manuscript; ARF performed the fieldwork; JCS reviewed the manuscript and acquired the financial resources of this research. All authors discussed the results and approved the final version of the manuscript.

